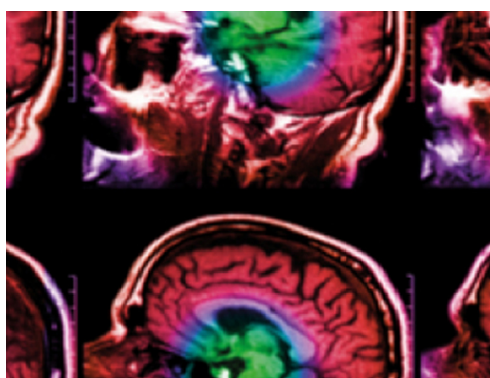


PAPER • OPEN ACCESS

# Analysis of the validity of the mathematical assumptions of electrical impedance tomography for human head tissues

To cite this article: Toby Williams *et al* 2021 *Biomed. Phys. Eng. Express* **7** 025011

View the [article online](#) for updates and enhancements.



**IPEM | IOP**

Series in Physics and Engineering in Medicine and Biology

Your publishing choice in medical physics,  
biomedical engineering and related subjects.

Start exploring the collection—download the  
first chapter of every title for free.

## Biomedical Physics &amp; Engineering Express



## PAPER

## OPEN ACCESS

RECEIVED  
28 July 2020

REVISED  
19 January 2021

ACCEPTED FOR PUBLICATION  
29 January 2021

PUBLISHED  
8 February 2021

Original content from this work may be used under the terms of the [Creative Commons Attribution 4.0 licence](#).

Any further distribution of this work must maintain attribution to the author(s) and the title of the work, journal citation and DOI.



## Analysis of the validity of the mathematical assumptions of electrical impedance tomography for human head tissues

Toby Williams<sup>1,\*</sup> , Kaddour Bouazza-Marouf<sup>1</sup>, Massimiliano Zecca<sup>1</sup> and Alexander L Green<sup>2</sup>

<sup>1</sup> Wolfson School of Mechanical, Electrical, and Manufacturing Engineering, Loughborough University, Leicestershire, LE11 3TU, United Kingdom

<sup>2</sup> Nuffield Department of Surgical Sciences, University of Oxford, Oxfordshire, OX3 9DU, United Kingdom

\* Author to whom any correspondence should be addressed.

E-mail: [t.williams@lboro.ac.uk](mailto:t.williams@lboro.ac.uk), [k.bouazza-marouf@lboro.ac.uk](mailto:k.bouazza-marouf@lboro.ac.uk), [m.zecca@lboro.ac.uk](mailto:m.zecca@lboro.ac.uk) and [alex.green@nds.ox.ac.uk](mailto:alex.green@nds.ox.ac.uk)

**Keywords:** Bioimpedance, Conductivity, Permittivity, Electrical Impedance Tomography (EIT)

Supplementary material for this article is available [online](#)

## Abstract

**Objective:** To determine the validity of the key mathematical assumptions used in electrical impedance tomography for human head tissues. **Approach:** Conductivity and permittivity data collected from available literature for each tissue within the human head have been evaluated and critiqued. The most relevant dielectric tissue data for each tissue was then used to assess the validity of the mathematical assumptions of electrical impedance tomography in terms of their suitability for human head imaging in order to estimate related errors. **Main Results:** For induced currents with frequencies greater than 200 Hz the internal current source density is negligible. The assumption that magnetic effects are negligible is valid to an error of 1.7% for human head tissues for frequencies below 1 MHz. The capacitive effects are negligible for CSF, dura mater, blood, bone (cortical), and deep tissue skin for frequencies less than 3.2 MHz, 320 kHz, 25 kHz, 3.2 kHz, and 130 Hz respectively. However, the capacitive effects are not negligible for brain tissues, as the minimum error for brain tissues across the frequency range of 10 Hz to 100 GHz is 6.2% at 800 Hz, and the maximum error is 410% at 20 GHz. **Significance:** It is often assumed that the mathematical reduction of the base equations is valid for human head tissues over a broad frequency range; this study shows that these assumptions are not true for all tissues at all frequencies. False assumptions will result in greater errors and local distortions within tomographic images of the human head using electrical impedance tomography. This study provides the relationships between injected current frequency and the validity of the mathematical assumptions for each individual tissue, providing greater awareness of the magnitude of possible distortions.

## 1. Introduction

Electrical impedance tomography (EIT) is a non-invasive, non-radiating and non-ionising technique capable of producing tomographic images of interior sections of a body. The technique involves injection of small alternating currents ( $\leq 10$  mA for medical applications) onto the surface of a body using electrocardiogram (ECG) type electrodes and measuring the resulting potentials around the surface (Nunez and Srinivasan 2006). Inhomogeneities that have a different conductivity compared to a homogeneous background cause the development of unique current

paths and specific sets of potential distributions. Voltage reading electrodes measure boundary potentials allowing for the tissue distribution within the body to be estimated.

The calculation used for the estimation of the conductivity distribution from known boundary voltage measurements is referred to as the inverse problem. The inverse problem is severely ill-posed and non-local, relying upon several forms of regularisation and *a priori* information to be able to reconstruct the conductivity distribution images. Therefore, a forward solution is first solved to provide an estimation of the boundary potentials that should be developed

supposing that the material distribution within the body is as anticipated. These predicted boundary potentials are then compared with the actual (measured) boundary potentials and the inverse solution is then used to minimize the error signal and generate an image of the anomalous conductivity distribution.

To solve the forward solution for EIT either a measurement of the boundary potentials of the body before the development of an anomaly is used, or an accurate model of the body is used in a computer simulation to estimate the boundary potentials (without an anomaly). For many medical applications however, neither of these options are practical due to large variations in shape and size of organ systems because of gender, age, ethnicity, etc. This has led to the use of multi-frequency EIT (MFEIT), whereby measurements at different frequencies are taken with the anomaly in place, then compared against one another to form the final conductivity distribution image. EIT relies on the differentiation of tissues; therefore, it is important to know how the bioimpedance of tissues alter over different frequency ranges. This is critical for both the development imaging algorithms and phantom tissue models used for development testing.

In order to determine the presence and location of an anomaly using EIT it is critical to understand the relationship between the admittivity and the electrical input frequency of the anomaly and its surrounding tissue. By knowing the change in conductivity of tissues between two known frequencies, each voxel of the change in conductivity matrix,  $\Delta \sigma$ , can be assigned an estimated tissue, whereby:

$$\Delta \sigma = A^\dagger \mathbf{V}, \quad (1)$$

$$\Delta \mathbf{V}_{FDA_i} = \mathbf{V}_{f_i} - \mathbf{V}_{f_{i-1}}, \quad (2)$$

where  $A^\dagger$  is the pseudo-inverse of the sensitivity matrix,  $\mathbf{V}$  is either the matrix of boundary voltages or the difference in boundary voltages between two frequencies,  $\Delta \mathbf{V}_{FDA_i}$  is the frequency difference adjacent matrix of boundary voltages for two subsequent frequencies and,  $\mathbf{V}_{f_i}$  and  $\mathbf{V}_{f_{i-1}}$  are boundary voltage matrices at frequencies  $f_i$  and  $f_{i-1}$  respectively.

This paper assesses the reliability of the measurement methods used and the agreement between data sets for published dielectric tissue data. The best published data are identified, based on their measurement methodologies and their agreement with other collected data, and used to assess the validity of the mathematical assumptions made in the formulation of the base equations for EIT in the identification of different tissues in the human head across a broad frequency range. Section 2 introduces the different types of dielectric measurement methods for tissue analysis, introduces the effect of a tissue's physiological condition on the measured dielectric results, and discusses the suitability of each dielectric data set available from the literature for each tissue constituting the human

head. Section 3 assesses the validity of the mathematical assumptions made for the EIT conductivity mapping for each biological tissue. Concluding remarks are given in Section 4 on the overall usability and reliability of existing published data as well as potential measurements to be undertaken to improve the understanding of the anisotropy of different tissues.

## 2. Dielectric properties of head tissues

The majority of *in vivo* experimental human tissue data has not been recorded for the whole desired bandwidth of frequencies that are employed by various EIT strategies. The majority of EIT systems operate within a bandwidth of 100 Hz to 1 MHz. Many experimental studies on human tissue have been conducted at either low frequencies close to or including dc, or in the GHz range. In these instances it is common to supplement live human tissue data with that of autopsy material or excised animal tissue, where live human tissue data is lacking or unobtainable.

In this section experimental results from relevant studies are reviewed and critiqued, with the aim to provide a compilation of the most relevant and accurate data for the frequency response of different tissues available.

### 2.1. Measurement methodology

There are different methods of conducting impedance analysis; these depend on the number of terminal electrodes used for the analysis, either two, three, or four electrodes. Both the two- and three-terminal methods record voltages on current carrying electrodes. However, both of these methods suffer in that the electrode-material contact impedance and electrode polarisation caused by the flow of current directly affects the bioimpedance measurement taken. The three-terminal method attempts to mitigate the effects caused by active current flow through a voltage read electrode by utilising a passive reference electrode, but is still relatively susceptible to current flow effects, based on the contact tissue's properties and non-uniformity between electrode materials. The four-terminal method records boundary voltages on two non-current carrying electrodes. This negates contact impedance errors if the input impedance of the voltage recording amplifiers is sufficiently high as to allow negligible current to be drawn across the recording electrodes (Horeish 2006). It is therefore, important to understand how the dielectric properties of biological tissues have been collected, as two-terminal data may have either not accounted for the presence of contact impedance, or incorrectly measured the effect of contact impedance in their results.

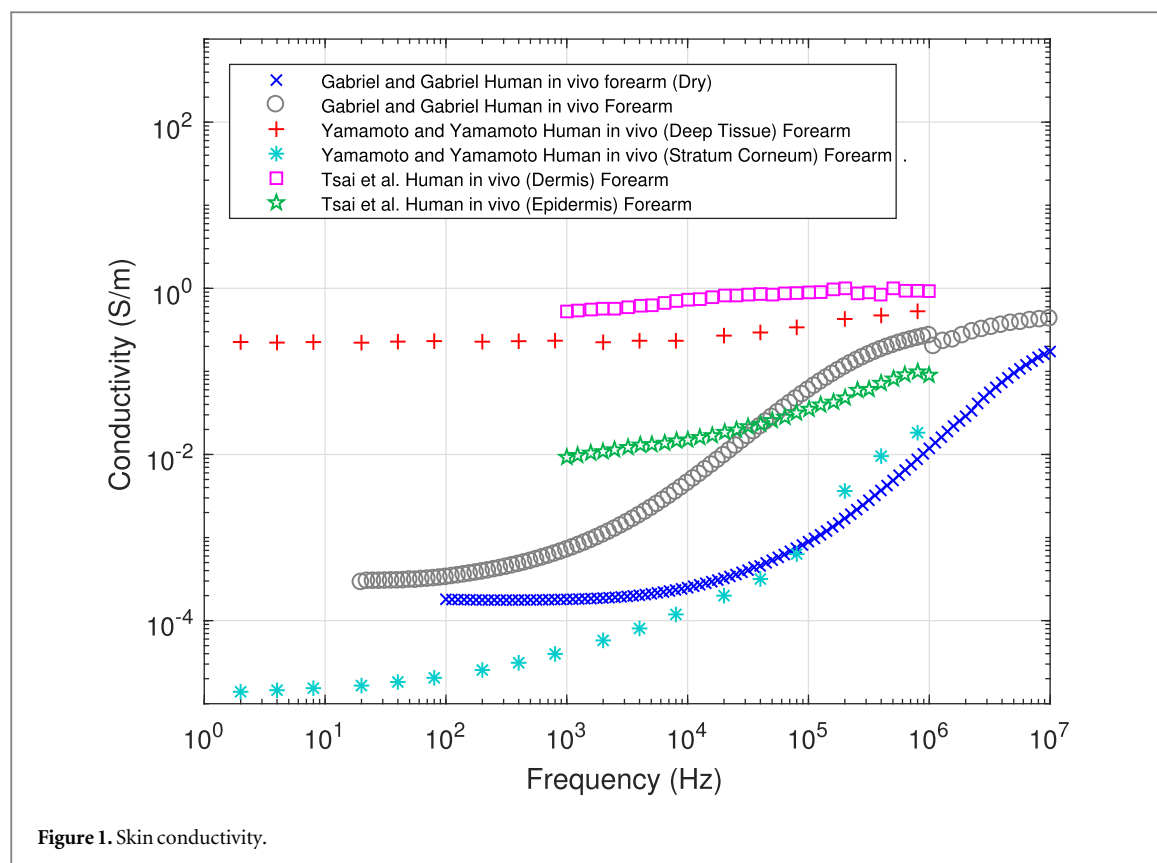


Figure 1. Skin conductivity.

## 2.2. Measurement environment and tissue condition

In general, it is not possible to take direct measurements of individual tissues *in vivo*. It is important that the excised tissue that measurements are taken from is in an environment that mimics that of being *in situ* in a live body as closely as possible (*ex vivo*).

It is also common for human autopsy materials to be used (Gabriel *et al* 1996a), especially for deep tissues and main organs. Once excised, it is important that the tissue be analysed as soon after removal/termination as possible, as cell death rapidly alters the internal structures of cells and organelles. It has been noted by Manwaring *et al* (2013) that during the euthanasia of piglets there was an immediate systematic decrease in global cerebral conductivity. The mean drop in conductivity before euthanasia and five minutes post-mortem was measured as  $12.6 \pm 13.2 \text{ mSm}^{-1}$  at 100 Hz. For comparison, the increase in conductivity before and after blood was injected into a section of the brain of anaesthetised piglets was measured as  $19.5 \pm 11.5 \text{ mSm}^{-1}$  (Manwaring *et al* 2013).

As very little data has been collected on the conductivity and permittivity for human tissues, mammalian tissue data is often utilised. The variation in a tissue's properties within a species may exceed the variation of that tissue's properties inter-species, depending on the tissue and the animal selected (Gabriel *et al* 1996). However, provided that a strong positive relationship may be shown over a limited frequency range, it can be assumed that non-human mammalian data

can provide a valid approximation (Gabriel *et al* 1996, Gabriel *et al* 1996a, Gabriel *et al* 1996b).

## 2.3. Head dielectric tissue properties

The human head is constituted of several distinct layers of biological tissue; skin, muscle, skull, cranial meninges, cerebrospinal fluid (CSF), and brain white and grey matter. In this section, each tissue's conductivity and permittivity data sets that are available from the literature are tabulated (Figures 1–11) as well as discussed and their suitability analysed.

It may be seen in the data tabulated in Figures 1–11, that there are regions that contain too much data and thus lack clarity; in these instances, additional graphs displaying the dielectrical trends in greater detail are given in the online supplementary material available (online at [stacks.iop.org/BPEX/7/025011/mmedia](https://stacks.iop.org/BPEX/7/025011/mmedia)).

### 2.3.1. Scalp

There have been several studies on the electric properties on the human skin, but no frequency dependent studies on the scalp have been undertaken. Although the properties of the skin are known to vary across the different parts of the body, significant data was only found to be available from the skin of the forearm.

The dielectric properties of skin are divided into two categories; dry and wet. As it is normal practice to use a conductive gel to reduce the affect of the resistive boundary layer effects between electrodes and the skin, the 'wet' properties of the skin are considered in this paper. For the dielectric properties of

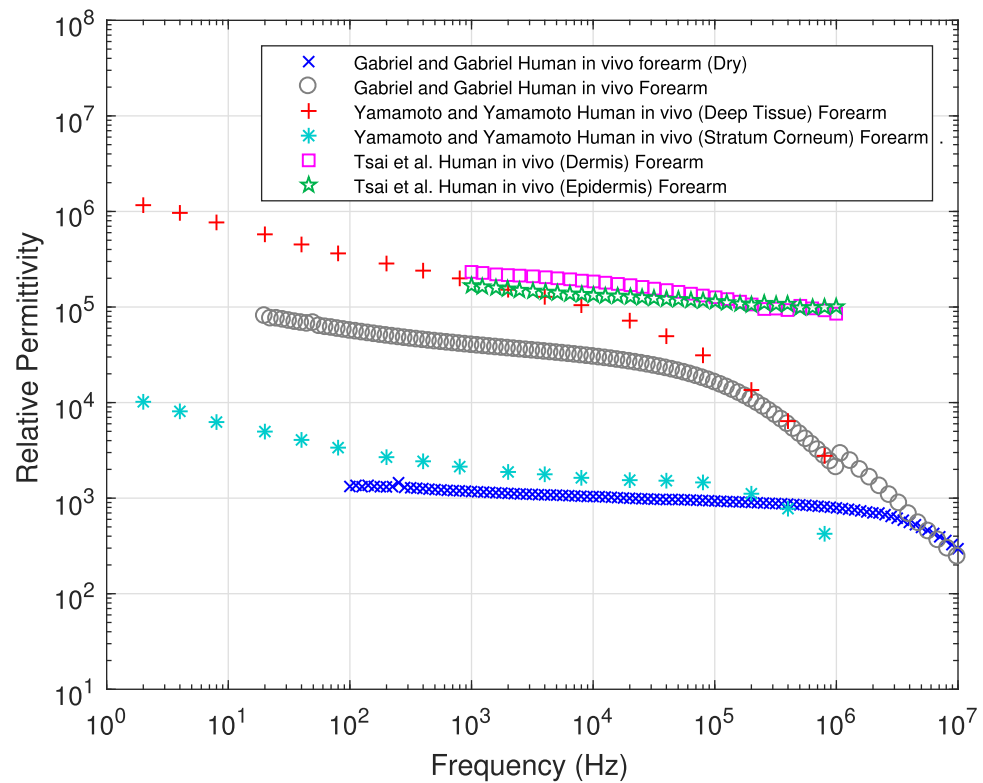


Figure 2. Skin relative permittivity.

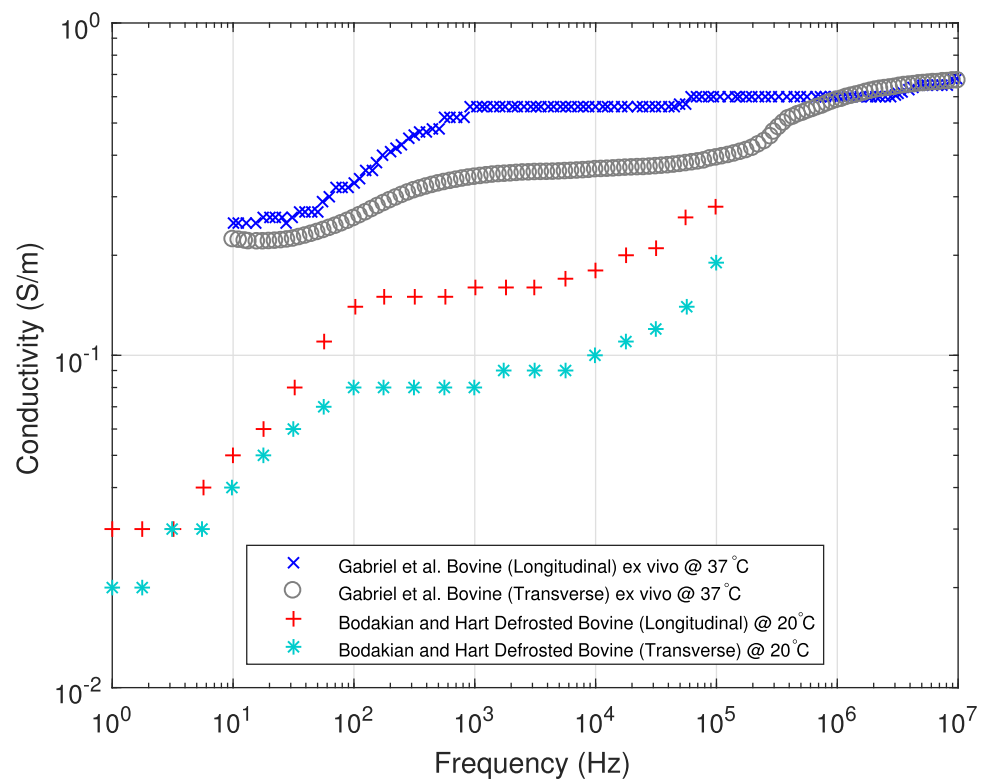


Figure 3. Muscle conductivity.

dry skin the following are recommended; (Grant *et al* 1988, Gabriel and Gabriel 1996, Tamyis *et al* 2005, Sasaki *et al* 2015).

Yamamoto and Yamamoto (1976) recorded the resistivity and permittivity of the skin of the forearm *in vivo* in the frequency range 2 Hz to 1 MHz. They measured the

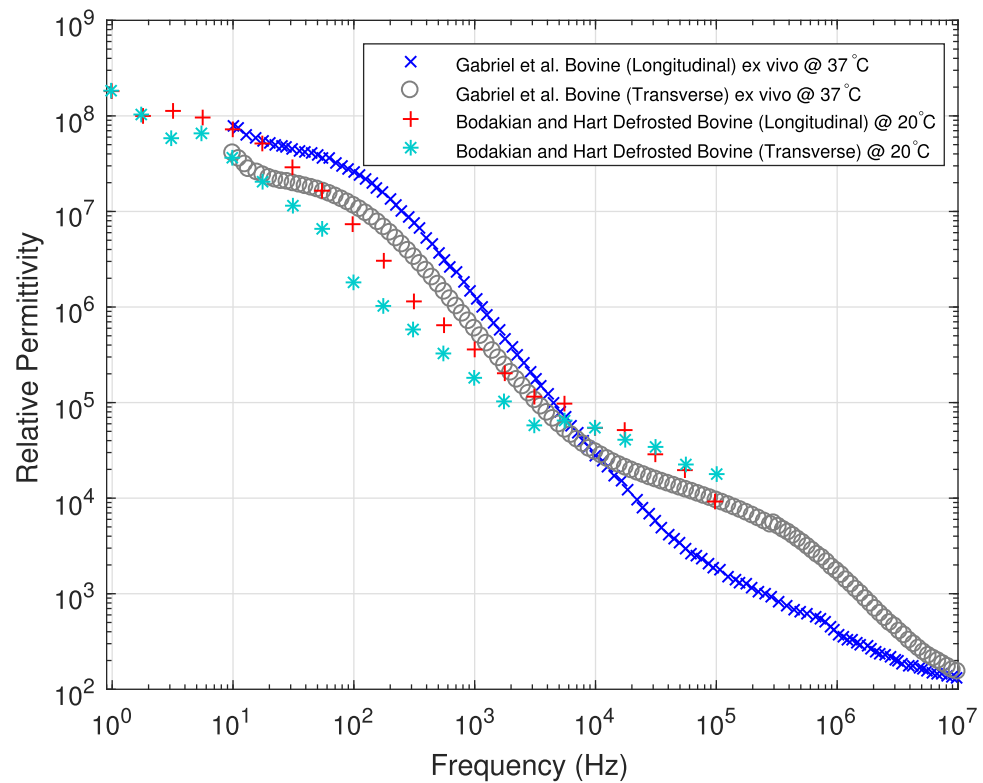


Figure 4. Muscle relative permittivity.

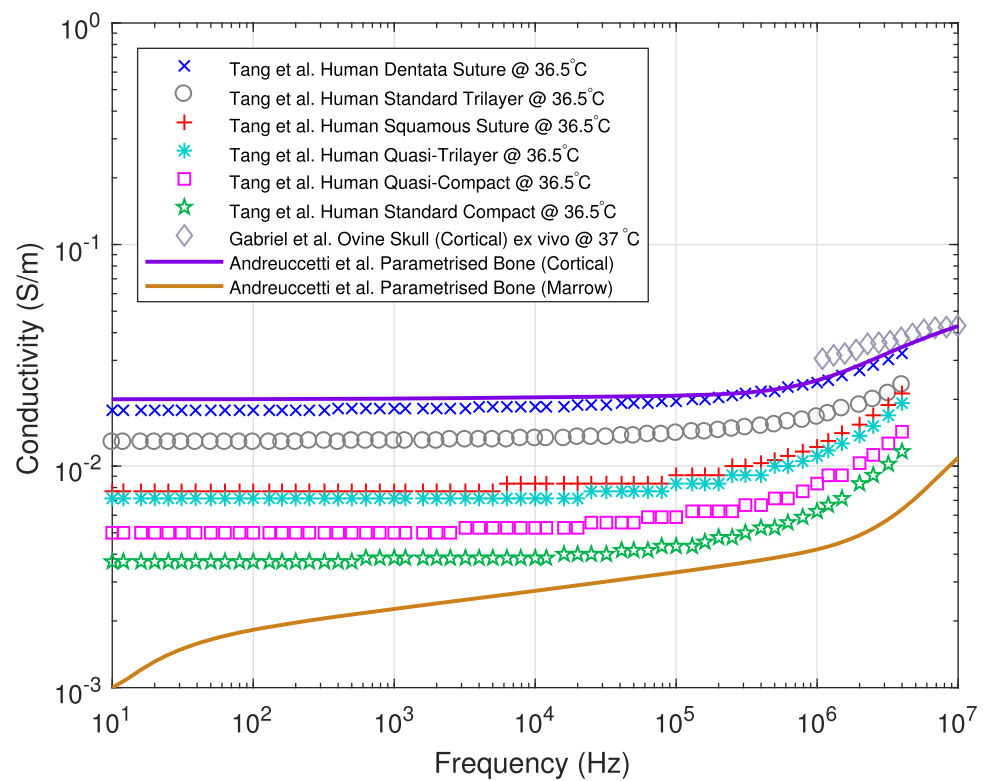


Figure 5. Skull conductivity.

electrical properties of the stratum corneum and deep tissue skin using the two terminal method and compensating for the effect of lead wire stray impedance and

electrode polarisation. Tsai *et al* (2019) also measured the dielectric properties of different layers of human forearm skin *in vivo* over the frequency range of 1 kHz to 1 MHz

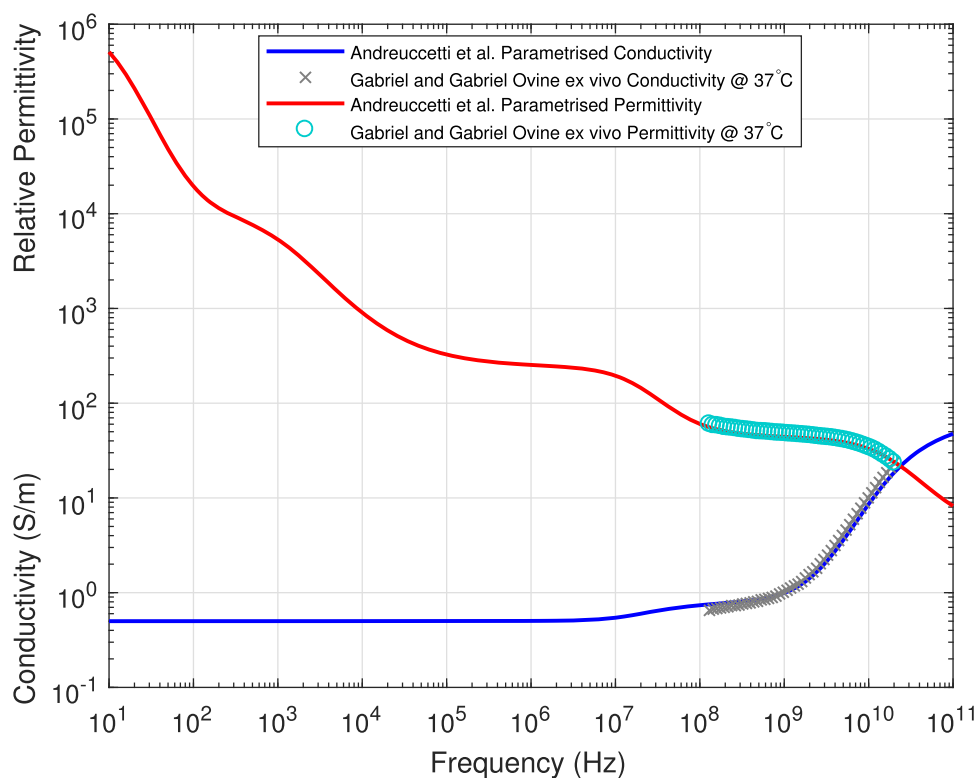


Figure 6. Dielectric properties of the dura mater.

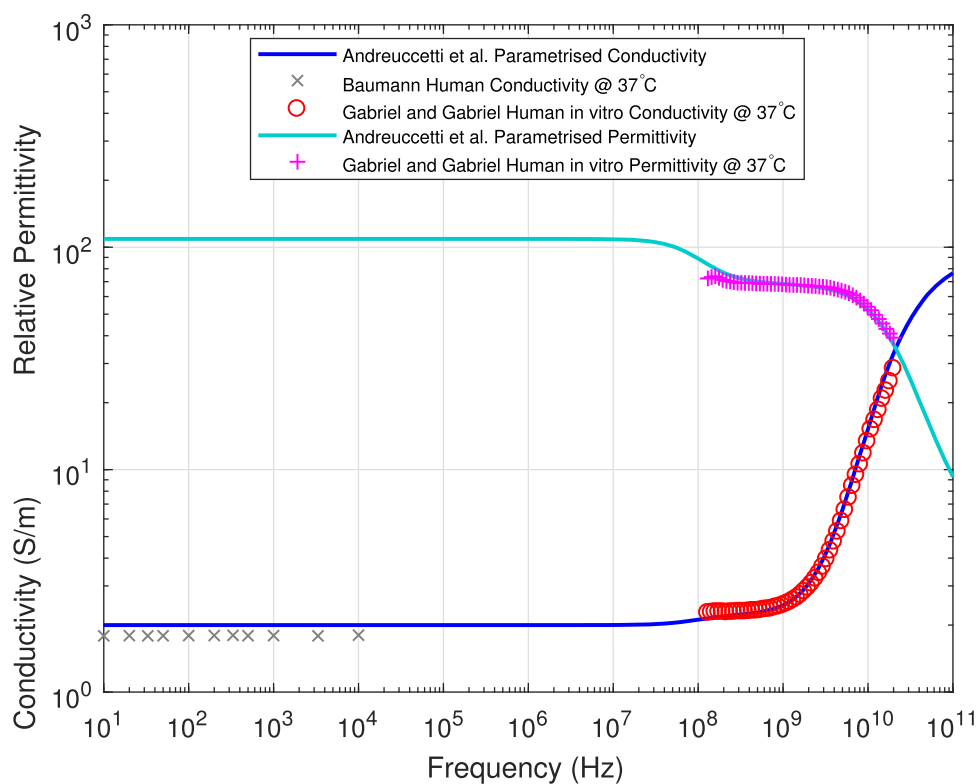
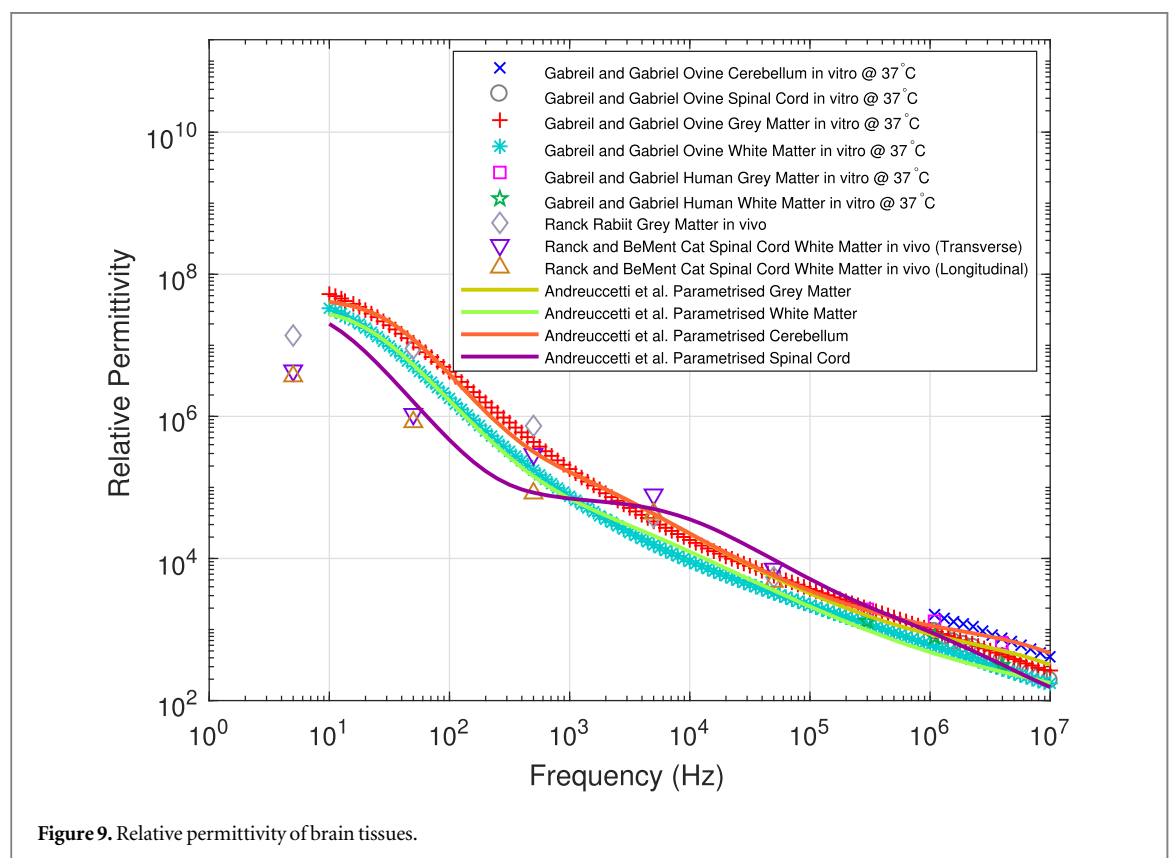
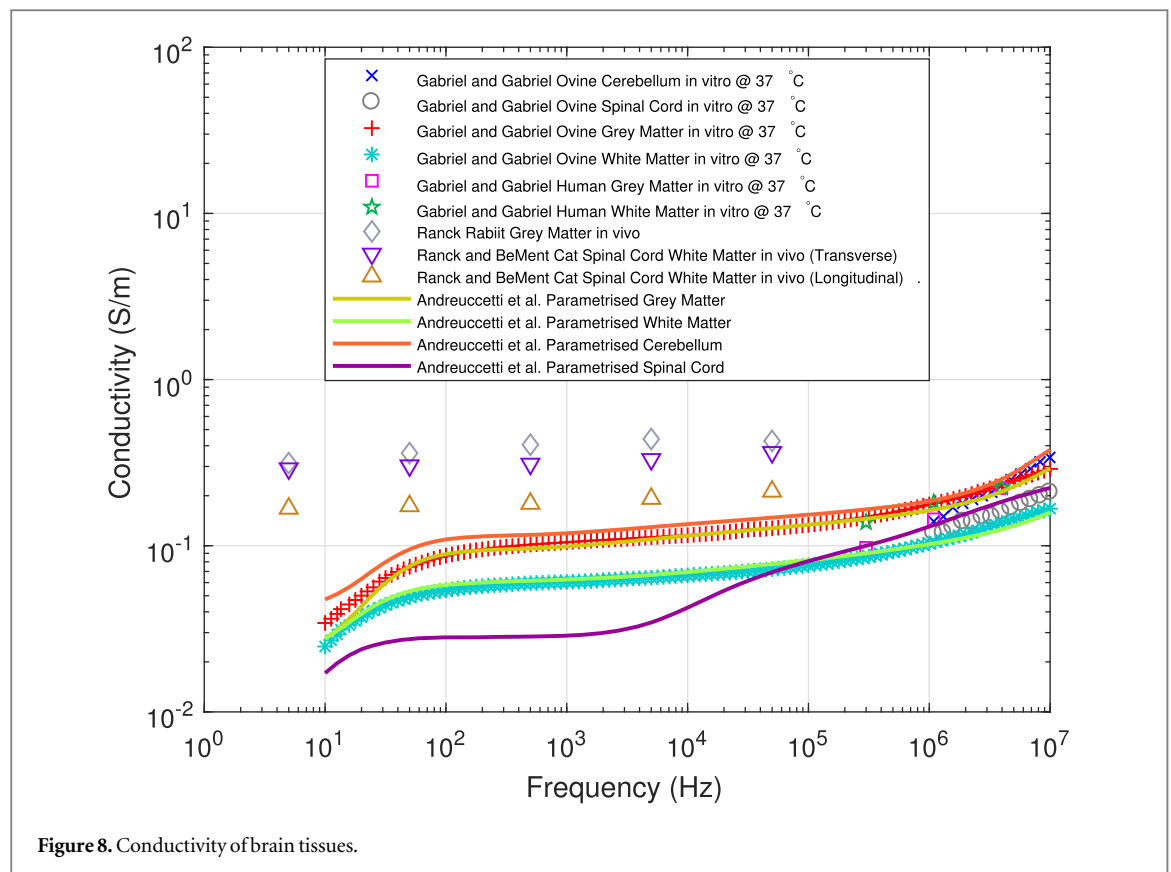


Figure 7. Dielectric properties of cerebrospinal fluid.

using the four-terminal method. They recorded measurements for the dermis and the epidermis by changing the effective current penetration depth of their recordings.

Gabriel and Gabriel (1996) conducted corrected two-terminal measurements on the skin of the forearm *in vivo* in both 'wet' and 'dry' conditions over a

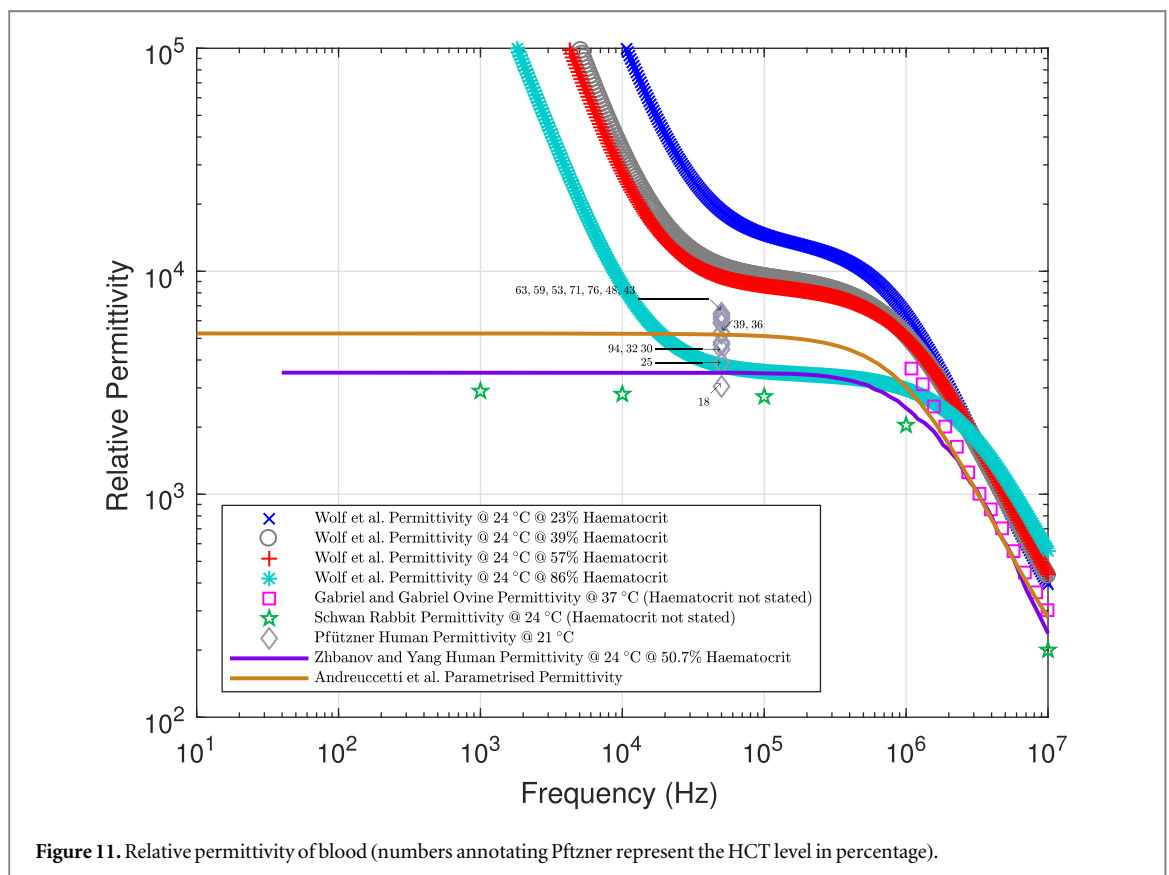
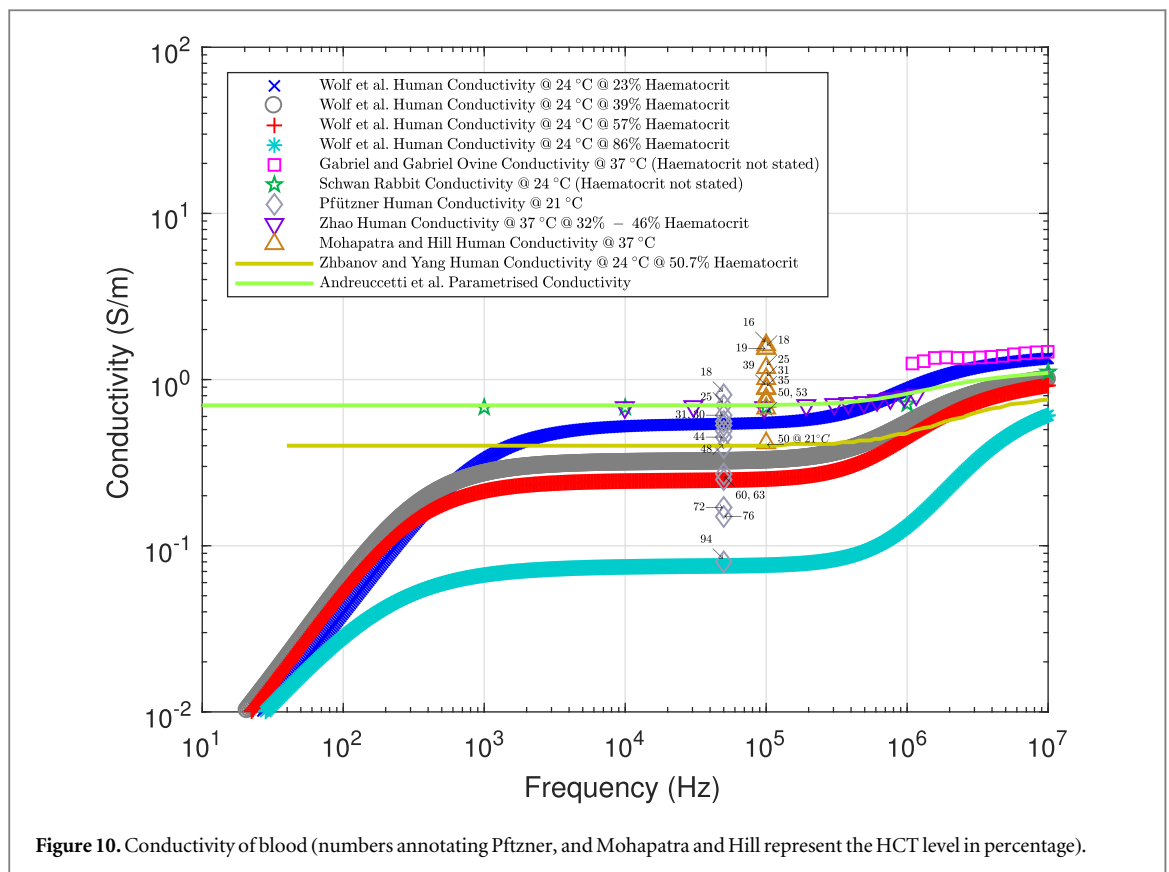




wide frequency range from 10 Hz to 20 GHz. They corrected their results to account for lead inductance and electrode polarisation.

Figure 1 shows the conductivity of skin (and location when identified) extracted from Gabriel and Gabriel (1996) and the conductivity derived from the resistivity





measurements of Yamamoto and Yamamoto (1976) and Tsai *et al* (2019). Figure 2 shows the permittivity of skin extracted from Yamamoto and Yamamoto (1976), Tsai *et al* (2019), and Gabriel and Gabriel (1996).

From Figures 1 and 2 it can be seen that the Yamamoto and Yamamoto deep tissue skin measurements converge with Gabriel and Gabriel wet skin measurements at above 100 kHz and diverge at lower

frequencies. This is to be expected between sets of measurements that include/exclude the stratum corneum, because at high frequencies a tissue's capacitive effects (susceptivity) dominate its behaviour, negating the effects of the stratum corneum's conductivity and permittivity.

As Yamamoto and Yamamoto recorded only a single measurement for the skin (bar the stratum corneum) it is to be expected that Tsai *et al* individual dermis and epidermis measurements would differ in magnitude to Yamamoto and Yamamoto's deep skin measurements, but agree in their trend. This is true for the conductivity, but Tsai *et al* permittivity measurements describe a much shallower decrease above 10 kHz then is shown by the other data sets.

### 2.3.2. Muscle

Muscle cells are much longer than they are thicker, giving muscle a very obvious anisotropic nature, longitudinally and transversely. There are several different muscle groups covering the skull overlaying one another and orientated in multiple directions. Muscle fibres, just like skin, are also expected to differ in their dielectric properties based on their location.

Gabriel *et al* (1996a) conducted corrected two-terminal measurements for the longitudinal and transverse conductivity and permittivity of bovine muscle *in vitro* at body temperature within two hours of death, over a frequency range of 10 Hz to 20 GHz. Bodakian and Hart (1994) examined the dielectric properties of longitudinal and transverse bovine muscles of defrosted samples at 20°C using the three terminal method.

Figures 3 and 4 show the dielectric properties of muscle tissue extracted from Bodakian and Hart (1994) and Gabriel *et al* (1996a).

It can be seen that the Gabriel *et al* measurements agree with the magnitude difference between the longitudinal and transverse muscle measurements of the defrosted bovine by Bodakian and Hart. The defrosted bovine muscle, Bodakian and Hart, is shown to be less conductive compared to fresh post mortem bovine muscle tissue by Gabriel *et al*. The non-agreement of results could be because the defrosted tissue was tested at 20°C instead of at body temperature (37°C), and it is probable that the processes of freezing and defrosting the tissue physically altered its cellular structure, changing its dielectric behaviour.

### 2.3.3. Skull

The most detailed and comprehensive study of skull bone is provided by Tang *et al* (2008). Skull samples were excised during surgery from 48 live patients (10 female and 38 male), aged between 20–74 years old. The resistivity of the samples were measured at 36.5°C over a frequency range of 1 Hz to 4 MHz. Measurements were taken for the six distinct skull sections of standard trilayer, quasi-trilayer, standard compact, quasi-compact, squamous suture, and dentate suture.

Gabriel *et al* (1994) conducted corrected two-terminal measurements on *ex vivo* ovine cortical skull bone at 37°C within two hours of death. The measurements were collected over a frequency range of 1 MHz to 20 GHz. Andreuccetti *et al* (1997) developed parametrically modelled data sets based on data published by Gabriel and Gabriel (1996) and Gabriel *et al* (1996, 1996a, 1996b); parametrically modelled data sets were developed for generic cortical and marrow bone based on several independent studies of human, mammalian, *in vivo* and *in vitro* bone and skull bone. This data set spans over 10 Hz to 20 GHz.

Figure 5 shows the conductivity as a function of frequency for skull bone extracted from Tang *et al* (2008), Gabriel *et al* (1994), and Andreuccetti *et al* (1997). Tang *et al* skull bone and suture characterisation is recommended for reference as their measurements took into account the different types of skull bone cross-sections from a large sample of male and female patients, treating the skull as inhomogeneous.

### 2.3.4. Cranial meninges

The brain is enclosed by the cranial meninges which consist of three protective layers: the pia mater, the arachnoid mater and the dura mater. No dielectric data can be found analysing the pia mater, arachnoid, or the cranial meninges. Only one study by Gabriel and Gabriel (1996) was found to contain dielectric data for large mammalian dura mater. Gabriel and Gabriel measured *ex vivo* ovine dura at 37°C within two hours of death. The data was collected over a frequency range of 130 MHz to 20 GHz; the data was then parametrically modelled and extrapolated over a frequency range of 10 Hz to 100 GHz by Andreuccetti *et al* (1997).

Figure 6 displays the change in dielectric properties for dura mater with respect to frequency extracted from Gabriel and Gabriel (1996) and Andreuccetti *et al* (1997).

### 2.3.5. Cerebrospinal fluid (CSF)

CSF is an ionic fluid with a low density of cells, with 0–5 cells/mm<sup>3</sup> normal for an adult (Martini 1998). As CSF is very conductive with no significant susceptibility (Baumann *et al* 1997), it can be assumed that *in vitro* measurements at body temperature should be representative of *in vivo* measurements.

Baumann *et al* (1997) recorded the conductivity of human CSF *in vitro* at 37°C using the four-terminal method between 10 Hz and 10 kHz. Gabriel and Gabriel (1996) measured *in vitro* human CSF at 37°C at between 24 to 48 hours postmortem. The measurements were collected over the frequency range of 130 MHz to 20 GHz; Andreuccetti *et al* (1997) parametrically modelled and extrapolated Gabriel and Gabriel's measurements over the frequency range of 10 Hz to 100 GHz.

The dielectric properties of CSF extracted from Gabriel and Gabriel (1996), Baumann *et al* (1997) and

Andreuccetti *et al* (1997) are shown graphically in Figure 7. Below 10 kHz, there is approximately 11% difference between Baumann *et al* conductivity measurements, which have an average value of 1.79 S/m, and Andreuccetti *et al* conductivity values, which have an average value of 2.00 S/m below 10 MHz. Baumann *et al* data was obtained using the four-terminal method for a frequency range of 10 Hz to 10 kHz, while Gabriel and Gabriel used the two-terminal method for their measurements that are the basis for Andreuccetti *et al* extrapolated data. Therefore, Baumann *et al* conductivity values should be considered to be more accurate.

### 2.3.6. Brain tissue

The adult brain is composed of a central region of white matter surrounded by a outer layer of grey matter. Grey matter is isotropic in its dielectric nature as opposed to the white matter which is constructed of bundles of nerve fibres that are very anisotropic. Therefore the orientation of the measuring electrodes has a significant effect on the measured dielectric property for white matter (Ranck and BeMent 1965).

Gabriel and Gabriel (1996) provide data with the broadest frequency range of measured white and grey matter of both human and large mammalian, and cerebellum and spinal cord of large mammalian. Gabriel and Gabriel measured the *ex vivo* ovine tissues at 37°C within two hours of death, and the *ex vivo* human tissue at 37°C at between 24 to 48 hours post mortem. Andreuccetti *et al* (1997) extrapolated data sets for the dielectric behaviour of the cerebellum and spinal cord from Gabriel and Gabriel's ovine measurements over the frequency range 10 Hz to 100 GHz. Andreuccetti *et al* also used Gabriel and Gabriel's ovine and human measurements and measurements from small mammalian subjects from other studies to create parametrised data sets for white and grey matter dielectric properties. The dielectric measurements of the aforementioned small mammals are in very strong agreement with the human and ovine results of Gabriel and Gabriel (1996). Ranck (1963) recorded the complex specific impedance of *in vivo* grey matter of two anaesthetised rabbits using the three-terminal method over the frequency range of 5 Hz to 50 kHz. Ranck and BeMent (1965) measured the complex specific impedance of *in vivo* white matter of the dorsal columns of five anaesthetised cats in both the longitudinal and transverse directions using the three-terminal method over the frequency range of 5 Hz to 50 kHz.

The conductivity and permittivity of brain tissues extracted from Gabriel and Gabriel (1996), Andreuccetti *et al* (1997), Ranck (1963), and Ranck and BeMent (1965) are shown in Figure 8 and Figure 9.

Figure 8 and Figure 9 also show that the Andreuccetti *et al* parametric approximations for conductivity and permittivity of white and grey matter, and spinal cord have good agreement with the ovine and human measurements from Gabriel and Gabriel. Ranck and

BeMent conductivity measurements of cat white matter in the longitudinal and transverse directions (Figure 8 and Figure 9) show the conductivity to be anisotropic and the permittivity to be isotropic in nature. The conductivity measurements of white matter in Figure 8 show that on average the conductivity is 73% lower in the longitudinal than the transverse direction. However, the permittivity measurements in Figure 9 show largely isotropic behaviour for the white matter. The Ranck and BeMent cat white matter permittivity measurements are in agreement with the trend of the Andreuccetti *et al* parametric approximation for human white matter.

### 2.3.7. Blood

The dielectric properties of blood vary dramatically based on its condition and composition. The dielectric properties depend upon the blood temperature, haematocrit (HCT) level (the percentage of red blood cells to blood by volume), flow rate, and whether the blood is whole or haemolysed (Hirsch *et al* 1950, Mohapatra and Hill Mohapatra and Hill 1975, Pfützner Pfützner 1984). The range of normal HCT levels for adults is from 40% to 54% for human males and 37% to 47% for females (Horeh 2006).

Zhao *et al* (1993) used the four-terminal method to measure the conductivity of human blood at body temperature of 24 patients with HCT levels over the range of 32%–46%, over a frequency range of 10 kHz to 1.2 MHz. Gabriel and Gabriel (1996) recorded the dielectric properties of ovine blood *ex vivo* at 37°C within two hours of death between 1.09 MHz and 20 GHz. Andreuccetti *et al* (1997) extrapolated data sets for the dielectric behaviour of blood from Gabriel and Gabriel's ovine measurements and other mammalian tissue to produce calculated trends over the frequency range of 10 Hz to 100 GHz. Schwan (1963) measurements of rabbit blood is one of the studies used by Andreuccetti *et al* for defining the parametric model at low frequencies. The rabbit blood was measured *in vitro* at room temperature between 1 kHz and 10 MHz, however, the HCT level of the blood was not stated by Schwan.

Mohapatra and Hill (1975) measured the resistivity of human blood *in vitro* at 100 kHz using the two-terminal method with electrode polarisation corrections over a temperature range 22°C to 40°C and a HCT range 16% to 52.5%. Pfützner (1984) recorded the dielectric properties of human and porcine blood *in vitro* at 50 kHz and 21°C using the two-terminal method with raster electrodes over a HCT range of 94% to 18%. Pfützner's work shows that as HCT level decreases admittivity (conductivity) increases and permittivity decreases, and that the admittivity of human and porcine blood are comparable at 50 kHz.

Wolf *et al* (2011) measured the dielectric properties of human blood from a single patient at 37°C over the frequency range of 1 Hz to 40 GHz at HCT levels between 23% and 86%. Wolf *et al* used the two-

terminal method with a coaxial probe, but did not correct for electrode polarisation or compensate for stray capacitance. Zhanov and Yang (2017) performed dielectric testing on donated human blood that had been artificiality altered to a HCT of 50.7% at room temperature over a frequency range of 40 Hz to 110 MHz. The samples were measured with the two-terminal method using an impedance analyser with the results being corrected for electrode polarisation and stray impedance.

Figures 10 and 11 display the conductivity and permittivity of blood respectively extracted from the aforementioned papers. For each data set presented for the conductivity and permittivity in Figure 10 and Figure 11 respectively the blood HCT level is stated if given, and for the measurements of Mohapatra and Hill, and Pftzner the specific blood HCT of each data point is annotated as a percentage value (the percentage sign is not shown for clarity).

In Figure 10 Pfützner's 21°C measurements at 50 kHz agree with the measurements of: Wolf *et al* at 24°C at 86% HCT with Pfützner's 94% HCT, Wolf *et al* at 24°C at 57% HCT with Pfützner's 63% HCT, Zhanov and Yang at 24°C at 50.7% HCT and Mohapatra and Hill at 21°C at 50% HCT with Pfützner's 48% HCT, and Wolf *et al* at 24°C at 23% HCT with Pfützner's 30% HCT. Mohapatra and Hill's measurement at 37°C at 50% HCT at 100 kHz agree with the measurements of Zhao at 37°C at between 32% to 46% HCT and Schwan's rabbit blood at 24°C and the parametrised data from Andreuccetti *et al*

Figure 11 shows that there is less agreement between the HCT of blood and its permittivity than its conductivity. Wolf *et al* 24°C measurements at 50 kHz at 86% HCT agree with Zhanov and Yang's measurements at 24°C at 50.7% HCT and Pfützner's 21°C measurement at between 25% and 18% HCT. The effect of not compensating for electrode polarisation using the two-terminal method is evident in both Figure 10 and Figure 11 in the Wolf *et al* data sets below 10 kHz and 100 kHz for the conductivity and permittivity measurements respectively, as opposed to the measurements of Zhanov and Yang, Schwan, and Zhao that maintain a constant value at these low frequencies. The set of results that are deemed most representative of the dielectric behaviour of human blood at body temperature (37°C), 40%-50% HCT, and taking into account electrode polarisation is the parametric data sets by Andreuccetti *et al* Their results agree with the general magnitude and trend of the data sets that compensate for electrode polarisation at lower frequencies at 37°C in both Figure 10 and Figure 11, as discussed in the text above.

The normal range of HCT levels for human adults is 37% to 52% (Horesh 2006). The corresponding conductivity values are  $0.89 \text{ Sm}^{-1}$  and  $0.68 \text{ Sm}^{-1}$  respectively; these are extrapolates from Mohapatra and Hill's results taken at 37°C. This gives an expected percentage change of 75% between the HCT levels of

38.5% and 52.5% at 37°C at frequencies below 1 MHz for the conductivity of human blood.

### 3. Assessment of the mathematical assumptions for EIT

The governing equation of EIT is derived from Maxwell's equations. In order to derive it, several assumptions are made about the cellular structure and dielectric properties of all the tissues. Two of Maxwell's equations that are used in the derivation of the governing equation are Faraday's law of induction and Coulomb's law given below in (3) and (4) respectively; where  $\mathbf{E}$  is the electric field,  $\mathbf{B}$  is the magnetic flux,  $t$  is time,  $\mathbf{H}$  is the magnetic field,  $\mathbf{D}$  is the electric displacement, and  $\mathbf{J}$  is the electric current density:

$$\nabla \times \mathbf{E} = -\frac{\partial \mathbf{B}}{\partial t}, \quad (3)$$

$$\nabla \times \mathbf{H} = \frac{\partial \mathbf{D}}{\partial t} + \mathbf{J}. \quad (4)$$

Using the current assumptions that for each biological tissue:

- (i) The tissue is a linear isotropic medium
- (ii) The internal current source density is negligible at the induced measurement frequency,  $\mathbf{J}_s \approx 0$
- (iii) The tissue is a non-dispersive medium and that magnetic effects are negligible,  $\omega \mu \mathbf{H} \approx 0$
- (iv) The tissue is a conductive medium (i.e.  $\mathbf{J}_c = \sigma \mathbf{E}$ ), and the capacitive effects  $\omega \epsilon$  are negligible

(3) and (4) may be expanded to Maxwell's time harmonic equations, (5) and (6) respectively; where  $j$  is the unit imaginary number,  $\omega$  is the angular velocity,  $\mu$  is the magnetic permeability, and  $\mathbf{J}_c$  is the conduction current density:

$$\nabla \times \mathbf{E} = -j\omega \mu \mathbf{H} \approx 0, \quad (5)$$

$$\nabla \times \mathbf{H} = j\omega \epsilon \mathbf{E} + \mathbf{J}_c = (\sigma + j\omega \epsilon) \mathbf{E} \approx \sigma \mathbf{E}. \quad (6)$$

As the curl of  $\mathbf{E}$  tends to zero in (5),  $\mathbf{E}$  is equivalent to a gradient of a scalar,  $\mathbf{E} \equiv -\nabla \phi$ , where the scalar  $\phi$  is the electric potential. Substituting for  $\mathbf{E}$  in (6) and taking the divergent of both sides reduces (6) to a single second order elliptic partial differential equation, (7), noting that the divergence of a curl of a vector is equal to zero (i.e.  $\nabla \cdot (\nabla \times \mathbf{H}) \equiv 0$ ). Equation (7) is often referred to as the governing equation of EIT and allows for the calculation of the electric potential  $\phi$  once the boundary conditions are defined.

$$\nabla \cdot (\sigma \nabla \phi) = 0. \quad (7)$$

By using the governing equation (7), the user implicitly assumes that the above assumptions (i) to (iv) are valid, which is not always true for every biological tissue at every frequency. Therefore, it is important to define the validity of the assumptions in



relation to the tissue(s) being investigated and the technique applied (e.g. the frequency range used). The validity of each assumption is discussed below for human head tissues.

### 3.1. Linear isotropic medium assumption

This assumption is not true for all of the tissues that constitute the human head. Scalp, muscle, skull, and white matter are known to be anisotropic. The anisotropic nature of muscle has been relatively well documented, but for scalp, skull, and white matter less information is available. It is unclear how the anisotropic nature of the scalp and skull would affect the propagation of electrical current. However for white matter, which is the central internal tissue in the head, it can be assumed that its anisotropy is equally orientated, and therefore could be modelled globally as an isotropic tissue (Horesh 2006). Therefore, the assumption that human head tissues are linear isotropic mediums is not true for the scalp and skull tissues.

### 3.2. Internal current source density assumption

The electric current density is influenced by two factors, the conduction current density  $\mathbf{J}_c$  and the internal source current density  $\mathbf{J}_s$ . The total electrical current density  $\mathbf{J}$  is given as:

$$\mathbf{J} = \mathbf{J}_c + \mathbf{J}_s. \quad (8)$$

The activity of brain waves above 200 Hz are linked to the onset or presence of seizures and spasms (Hughes 2008). Therefore, externally injected current should be limited to above 200 Hz so not to be contaminated by internal sources during normal brain function. Thus, in EIT applications it is correctly assumed that  $\mathbf{J}_s \rightarrow 0$  at the induced measurement frequency ( $> 200$  Hz).

### 3.3. Assumption of negligible magnetic effects

It is often assumed that for biomaterial  $\omega\mu\mathbf{H} \approx 0$ . The quasi-static approximation states that this is valid only if (Nunez and Srinivasan 2006):

$$\frac{\omega\mu\sqrt{\sigma^2 + (\omega\epsilon)^2}}{K^2} \ll 1. \quad (9)$$

where  $K$  is the magnitude of the wavenumber vector. The left hand side (LHS) of (9) is defined as the ratio between magnetic induction and the conductive effects. As biological tissues are non-metallic the permeability of each tissue can be assumed to be the permeability of free space,  $\mu \approx \mu_0 = 1.257 \times 10^{-6} \text{ Hm}^{-1}$ .

Assuming that the tissues are non-dispersive lossless mediums, the magnitude of the wavenumber vector is calculated as:

$$K = \frac{2\pi}{\lambda}. \quad (10)$$

where  $\lambda$  is the characteristic spatial wavelength. Thus, the ratio in (9) is directly proportional to  $\lambda^2$ . Therefore,

a large value of  $\lambda$  will result in a conservative approximation of the ratio in (9) with respect to the upper limit of 1 (Nunez and Srinivasan 2006).

Bushby *et al* (1992) recorded the heights and head diameters of 354 white adults, finding that the head diameter is proportional to height. The 97th percentile of head diameter for men with a height of 200 cm was found to be 62.4 cm. As an overestimation, a head diameter of 65 cm has been used to calculate a characteristic spatial wavelength of 0.207 m, resulting in a wavenumber vector magnitude of  $30.4 \text{ m}^{-1}$  (Nunez and Srinivasan 2006).

Using the above value of  $K$  and the dielectric behaviour of each tissue described in Section 2 (using generic bone data instead of skull bones due to a lack of skull permittivity data), the ratio in (9) is plotted against frequency in Figure 12.

It can be seen in Figure 12 that the ratio in (9) of all the tissues remains below 0.01 up to 600 kHz, 0.017 up to 1 MHz, and 0.1 up to 6 MHz. Therefore, the assumption that the magnetic induction is negligible is a very good approximation at frequencies less than 1 MHz, with the assumption becoming less valid at higher frequencies.

### 3.4. Assumption of negligible capacitive effects

It is often assumed that the capacitive effects ( $\omega\epsilon\mathbf{E}$ ) are negligible compared to the conductive effects within biological tissues. This assumption requires that a tissue's admittivity,  $\gamma$ , is equivalent to its conductivity, i.e.  $\gamma \approx \sigma$ . Admittivity is the combined effects of the real conductivity and the imaginary susceptibility, given as:

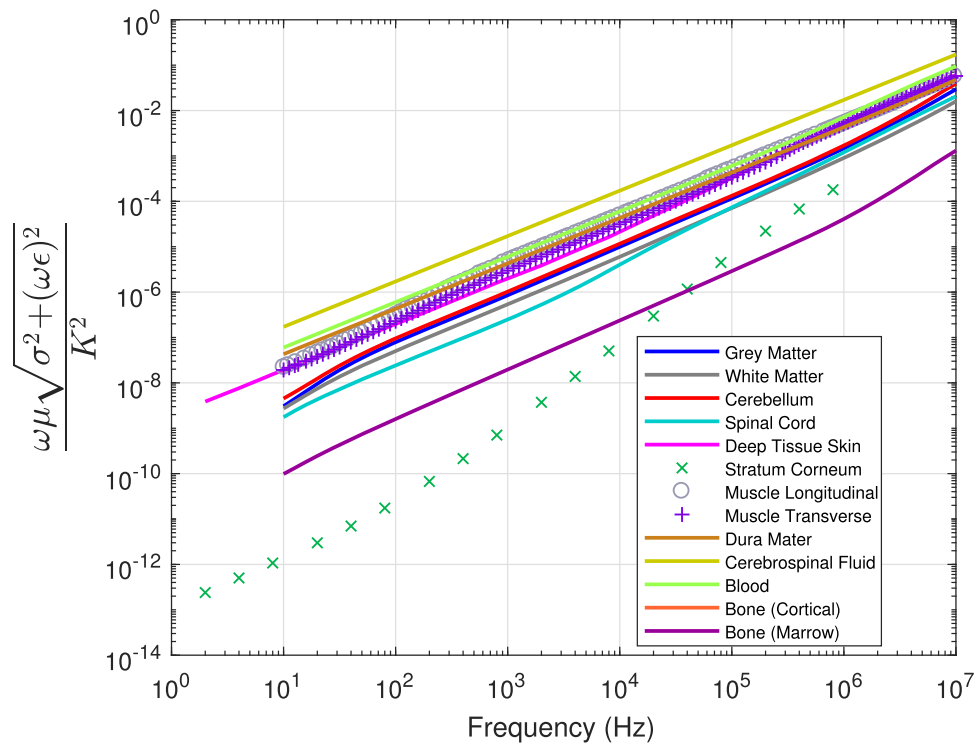
$$\gamma = \sigma + j\omega\epsilon. \quad (11)$$

If it is assumed that admittivity is equivalent to conductivity, by dividing (11) by  $\sigma$  it is clear that the ratio of susceptibility and conductivity must be much less than one for the quasi-static approximation of negligible capacitive effects to be valid.

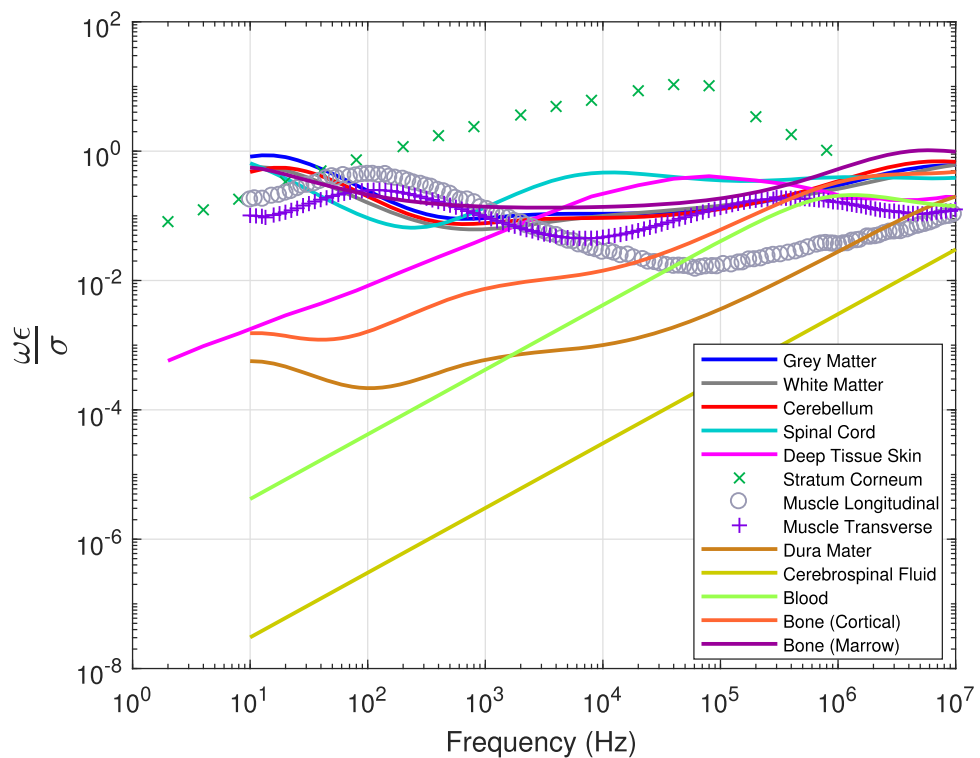
$$\frac{\omega\epsilon}{\sigma} \ll 1. \quad (12)$$

Figure 13 displays the ratio in (12) applied to the tissues described previously in this paper (as used in assumption 3 above).

Figure 13 shows that bar the stratum corneum the ratio for all the tissues remains below 1 for frequencies less than 10 MHz, with the minimum ratio of 0.14 at 1 kHz. Figure 13 also shows that the assumption of negligible capacitive effects is valid for some tissues, but not for others, specifically not for brain tissue. For example, the minimum ratio for brain tissues is that of the white matter which is 0.062; while the ratio for CSF, dura mater, blood, bone (cortical), and deep tissue skin is below 0.01 at frequencies less than 3.2 MHz, 320 kHz, 25 kHz, 3.2 kHz and 130 Hz respectively. Therefore, it is questionable, specifically for head tissues, as to the validity of the assumption that the effect



**Figure 12.** Evaluation of the magnetic quasi-static approximation.



**Figure 13.** Evaluation of the capacitive quasi-static approximation.

of capacitance is negligible, as across the given frequency spectrum the majority of the tissues, at any given frequency, cannot be described as significantly less than 1.

#### 4. Discussion and conclusions

A study of the dielectric properties of human head tissues has been undertaken to investigate the validity

of the key mathematical assumptions used in EIT. Accurate images of the conductivity map generated from EIT relies on accurate data to describe the dielectric behaviour of the materials under analysis. Thus, without a complete understanding of the effect the electrical responses of the human head tissues on the assumptions made for EIT, there is a potential for significant errors to occur. This is of increasing concern with regard to medical applications as false-negative or false-positive results may have severe consequences.

The most relevant dielectric tissue data for tissues constituting the human head have been evaluated and critiqued for their suitability. The dielectric data have been used to assess the validity of the mathematical assumptions of EIT in terms of their suitability for human head imaging.

Andreuccetti *et al* (1997) maintain an online database of mathematically modelled dielectric properties of human tissues based on measurements and models of human and mammalian tissues by Gabriel and Gabriel (1996), Gabriel *et al* (1996, 1996a, 1996b), and others. This database gives very good approximations of tissue data and trends in general, but does not give data for local variations, such as scalp and flat muscle, or differentiation between the white and grey matters of different regions of the brain. Regions of the same tissue across the body are known to differ in their structural make-up depending on their location and, therefore, their dielectric behaviours are expected to differ also. Thus, Andreuccetti *et al* calculated data sets should be used with caution.

The main recommendations that describe the dielectric behaviour of each tissue are summarised below. In addition, graphical representation of the recommended data sets of the head tissues are supplied in the supplementary material.

- The scalp can be represented by forearm human skin measurements by Gabriel and Gabriel (1996) above 1 MHz, and below 1 MHz as a single entity by the forearm deep tissue skin measurements by Yamamoto and Yamamoto (1976) and as the dermis and epidermis separately between 1 kHz and 1 MHz by Tsai *et al* (2019).
- Muscle, transverse and longitudinal, can be represented by the bovine measurements by Gabriel *et al* (1996a).
- The skull conductivity can be represented by the human measurements of Tang *et al* (2008) below 4 MHz, which take into account the inhomogeneity of the skull, and the ovine cortical skull measurements by Gabriel *et al* (1994) above 4 MHz.
- The dura mater, CSF, grey matter, white matter, cerebellum, spinal cord, and blood at around 50%–52% HCT can be represented by the calculated tissue behaviours by Andreuccetti *et al* (1997).

The tissues analysed in this paper indicate that the assumption that internal current source density is negligible at the induced measurement frequency, and the assumption that magnetic effects are negligible, are valid to an error of 1.7% for human head tissues over the frequency range of 200 Hz to 1 MHz. The assumptions of negligible capacitive effects and isotropic tissues do not hold true for all human head tissues without introducing significant error. The scalp, muscle, skull, and white matter are known to be anisotropic. Abascal (2007) noted a 50% error in boundary voltages between two computer simulations, where one simulation accounted for the estimated anisotropy of the brain, skull and scalp, and the other did not.

EIT in its current form cannot be expected to give accurate results for the application of human head imaging without considering capacitive effects and obtaining a greater understanding of the anisotropy of the tissues. However, if complex admittivity was utilised in lieu of just the real part (conductivity) in defining the governing equation, (7), EIT could be expected to give valid results up to 1 MHz depending on the magnitude of the effect that anisotropy has on the scalp, muscle, and skull tissues.

In order to mitigate the effect of the errors caused by the assumption that human head biological tissues are homogeneous and isotropic, more measurements of the skin, scalp, muscle, and white matter are required to be undertaken to increase the knowledge of how these tissues behave over a range of frequencies. This is also true of blood; it is necessary to understand how variations of blood HCT level affect the conductivity and permittivity in frequencies above the steady state condition (<100 kHz). Research should also be conducted on the possibility of using admittivity to define the governing equation instead of conductivity to reduce the errors incurred by using the false assumption of negligible capacitive effects on human head tissues.

## Data availability statement

The data that support the findings of this study are available upon reasonable request from the authors.

## ORCID iDs

Toby Williams  <https://orcid.org/0000-0002-7162-2507>

Massimiliano Zecca  <https://orcid.org/0000-0003-4741-4334>

## References

- Abascal J F P 2007 *Improvements in reconstruction algorithms for electrical impedance tomography of brain function* University of London
- Andreuccetti D, Fossi R and Petrucci C 1997 "An internet resource for the calculation of the dielectric properties of body tissues in the frequency range 10 Hz—100 GHz". IFAC-CNR, Florence (Italy), 1997. Based on data published by C. Gabriel *et al.* in 1996. [Online]. Available: <http://niremf.ifac.cnr.it/tissprop/>



- Baumann S B, Wozny D R, Kelly S K and Meno F M 1997 The electrical conductivity of human cerebrospinal fluid at body temperature *IEEE Trans. Biomed. Eng.* **44** 220–3
- Bodakian B and Hart F X 1994 The dielectric properties of meat *IEEE Trans. Dielectr. Electr. Insul.* **1** 181–7
- Bushby K M D, Cole T, Matthews J N S and Goodship J A 1992 Centiles for adult head circumference *Archives of Disease in Childhood* **67** 1286–7
- Gabriel C, Chan T Y A and Grant E H 1994 Admittance models for open ended coaxial probes and their place in dielectric spectroscopy *Phys. Med. Biol.* **39** 2183–200
- Gabriel C and Gabriel S 1996 *Compilation of the dielectric properties of body tissues at RF and microwave frequencies* <http://www.dtic.mil/dtic/tr/fulltext/u2/a305826.pdf>
- Gabriel C, Gabriel S and Corthout E 1996 The dielectric properties of biological tissues: I. Literature survey *Phys. Med. Biol.* **41** 2231–49
- Gabriel S, Lau R W and Gabriel C 1996a The dielectric properties of biological tissues: II. Measurements in the frequency range 10 Hz to 20 GHz *Phys. Med. Biol.* **41** 2251–69
- Gabriel S, Lau R W and Gabriel C 1996b The dielectric properties of biological tissues: III. Parametric models for the dielectric spectrum of tissues *Phys. Med. Biol.* **41** 2271–93
- Grant J P, Clarke R N, Symm G T and Spyrou N M 1988 In vivo dielectric properties of human skin from 50 MHz to 2.0 GHz *Phys. Med. Biol.* **33** 607–12
- Hirsch F G, Texter E C, Wood L A, Ballard W C, Horan F E and Wright I S 1950 The electrical conductivity of blood I: relationship to erythrocyte concentration *Blood* **5** 1017–35
- Horesh L 2006 *Some novel approaches in modelling and image reconstruction for multi-frequency electrical impedance tomography of the human brain* UCL (University College London)
- Hughes J R 2008 Gamma, fast, and ultrafast waves of the brain: Their relationships with epilepsy and behavior *Epilepsy and Behavior* **13** 25–31
- Manwaring P K, Moodie K L, Hartov A, Manwaring K H and Halter R J 2013 Intracranial electrical impedance tomography: A method of continuous monitoring in an animal model of head trauma *Anesthesia and Analgesia* **117** 866–75
- Martini F H 1998 *Fundamentals of Anatomy & Physiology* 4th edn. (London: Prentice Hall, Inc.)
- Mohapatra S N and Hill D W 1975 The changes in blood resistivity with haematocrit and temperature *European Journal of Intensive Care Medicine* **1** 153–62
- Nunez P L and Srinivasan R 2006 *Electric Fields of the Brain: The Neurophysics of EEG* 2nd edn. (Oxford: Oxford University Press)
- Pfützner H 1984 Dielectric analysis of blood by means of a raster-electrode technique *Med. Biol. Eng. Comput.* **22** 142–6
- Ranck J B Jr. 1963 Specific impedance of rabbit cerebral cortex *Exp. Neurol.* **7** 144–52
- Ranck J Jr. and BeMent S L 1965 The specific impedance of the dorsal columns of cat: An anisotropic medium *Exp. Neurol.* **11** 451–63
- Sasaki K, Mizuno M, Wake K and Watanabe S 2015 Measurement of the dielectric properties of the skin at frequencies from 0.5 GHz to 1 THz using several measurement systems *40th International Conference on Infrared, Millimeter, and Terahertz Waves (IRMMW-THz)* 40 (Hong Kong) 1–2
- Schwan H P 1963 Electric characteristics of tissues: A survey *Biophysik* **1** 198–208
- Tamyis N M, Ghodgaonkar D K, Taib M N and Wui W T 2005 Dielectric properties of human skin in vivo in the frequency range 20–38 GHz for 42 healthy volunteers *Proc. of the 28th URSI General Assembly* 28, 1–4
- Tang C, You F, Cheng G, Gao D, Fu F, Yang G and Dong X 2008 Correlation between structure and resistivity variation of the live human skull *IEEE Trans. Biomed. Eng.* **55** 2286–92
- Tsai B, Xue H, Birgersson E, Ollmar S and Birgersson U 2019 Dielectrical properties of living epidermis and dermis in the frequency range from 1 kHz to 1 MHz *Journal of Electrical Bioimpedance* **10** 14–23
- Wolf M, Gulich R, Lunkenheimer P and Loidl A 2011 Broadband dielectric spectroscopy on human blood *Biochimica et Biophysica Acta—General Subjects* **1810** 727–40
- Yamamoto T and Yamamoto Y 1976 Electrical properties of the epidermal stratum corneum *Med. Biol. Eng.* **14** 151–8
- Zhao T X, Jacobson B and Ribbe T 1993 Triple-frequency method for measuring blood impedance *Physiol. Meas.* **14** 145–56
- Zhbanov A and Yang S 2017 Electrochemical impedance spectroscopy of blood for sensitive detection of blood hematocrit, sedimentation and dielectric properties *Anal. Methods* **9** 3302–13